Crystallization in Miniemulsion Droplets

Rivelino Montenegro, Markus Antonietti, Yitzhak Mastai, and Katharina Landfester*

Max Planck Institute of Colloids and Interfaces, Research Campus Golm, 14424 Potsdam, Germany

Received: May 30, 2002; In Final Form: March 28, 2003

Undercooling and crystallization in stable nanodroplets with a narrow size distribution were analyzed using differential scanning calorimetry (DSC) measurements. Hexadecane droplets in water and NaCl solution droplets in petrolether were prepared using the miniemulsion process. It was found that the undercooling required to obtain crystallization in such droplets is significantly increased, compared to the bulk material: for the hexadecane droplets, a shift from 12 °C (bulk) to approximately −4 °C (droplets) is observed, and for the NaCl solution, a shift from −22 °C (bulk) to −46 °C (droplets) is observed. This is explained by the fact that, in miniemulsions, each droplet must be nucleated separately and the nucleation mechanism is shifted from heterogeneous to homogeneous nucleation. The undercooling additionally increases as the temperature decreases, which is explained with finite size effects for spinodal decompositions. The interfacial tension does not have any influence on the crystallization process. It was found that the crystallization rate in miniemulsion droplets is higher than that of the bulk and is proportional to the droplet size.

Introduction

The physical properties of liquids in small droplets can be significantly different from those in the bulk phase, because small particles have high surface-to-volume ratios and the potential for surface effects to dominate over bulk effects.[1] On the other hand, it has been known that a transformation from liquid oil to fat crystals remarkably influences the physical properties of the emulsions, such as emulsion stability, rheology, and appearance.[2] These physicochemical properties play an important role in the manufacture, storage, transport, and application of emulsions.[3] In addition, crystallization within micrometer-sized emulsions droplets has critical implications in both biological and materials science research, such as the synthesis of nanosized particles for catalysis, semiconductors, optoelectronics, and purification techniques. Despite this wide importance, crystallization in fluid nanostructures is just starting to be examined, which we attribute to the accessibility of model systems.

1. Melting and Crystallization in Droplets. In several experimental studies on small nanoparticles or material confined in small pores, a decrease of the melting point was observed.[4] Such shifts in melting temperature from the bulk transition can be understood on the basis of classical thermodynamical arguments, by balancing the bulk and interfacial contributions to the free energy of the solid and liquid phases. From the Gibbs−Thomson equation,

$$\Delta T_m = T_{mb} - T_m = \frac{2T_{mb}\gamma_{sl}\nu_1}{\Delta_{sl}H} \quad (1)$$

where T_{mb} and T_m respectively represent the bulk and droplet transition temperatures, γ_{sl} is the interfacial tension, ν_1 is the molar volume of the liquid, and $\Delta_{sl}H$ is the molar enthalpy of melting, a linear dependence of ΔT_m on the inverse droplet size is predicted. As a second possibility, additional additives within the particles can also lower the melting point.

The crystallization in emulsions with larger droplets has been studied extensively, and a theoretical analysis of the crystallization kinetics is now well established.[5−8] Recent studies focused on the use of such systems to modify crystallization to obtain favorable crystalline forms.[9,10] Contrary to a bulk system, in emulsions, one must create a large ensemble of independent nucleation sites and, after nucleation, the crystal growth is governed and limited by the size of the droplet and is stopped when the droplet border is reached.

The nucleation can be either homogeneous if the droplet is an ideally pure liquid, e.g., without any added components (nanoparticles or foreign molecules), or heterogeneous if added components are present, which behave as nucleating sites. It is known that homogeneous nucleation occurs at lower temperatures than heterogeneous nucleation.[11]

It is well-known that emulsification tends to increase the undercooling required for crystallization over that of bulk liquids. A reduction in the crystallization temperature, i.e., the temperature wherein a defined kinetic protocol crystallization occurs, has been reported by McClements et al.[12] and Kaneko et al.[2] In their opinion, the reason for the shifting in the crystallization temperature could be associated with the number of foreign crystallization nuclei that usually cause heterogeneous nucleation in the bulk phase and are now distributed among a large number of isolated droplets. Therefore, only a small number of droplets now contain such a foreign element for heterogeneous crystallization, and, therefore, the probability for heterogeneous nucleation for all the droplets is drastically reduced.[13]

The effect of added components or surfactant molecules on the nucleation in emulsion studies is not obvious. Clearly, one possible role is to act as heterogeneous nucleation sites, and Turnbull and Perepezko have discussed this. For example, in mercury, Turnbull showed that changes in the surfactant could increase the undercooling from 5 °C to 60 °C, but the melting was similarly influenced.

* Author to whom correspondence should be addressed. E-mail: landfester@mpikg-golm.mpg.de

10.1021/jp0262057 CCC: $25.00
Published on Web 05/02/2003

The nucleation rate is strongly temperature dependent; for example, in *n*-alkanes, the nucleation rate can change by a factor of 5000 per degree celsius. The size of the emulsion droplets also plays a key role in nucleation studies. In homogeneous nucleation, the nucleation rate is proportional to the volume of the droplets. Typically, the determination of the size distribution for the emulsions is a large source of errors in nucleation-rate measurements.

Few groups have studied the alkane nucleation through the use of emulsion samples. The earliest work is from Turnbull and Cormia,[6,7] who studied C-16, C-17, C-18, C-24, and C-32 alkanes. They noted that there seemed to be an unusual spread in the melting temperatures, and that a second anomaly—the reduced undercooling—is observed in those studies. The reduced undercooling is defined as $\Delta T = (T_m - T_n)/T_n$, where T_n is the point where the nucleation rate becomes significant in the emulsion samples and T_m is the thermodynamic melting temperature. Other groups[14,15] who were studying nucleation in emulsions focused on the behavior of C-16, using ultrasound transmission to measure the proportion of the liquid to solid in an emulsion sample. Their results exhibit the typical 14−15 °C undercooling, as also found by other workers. The nucleation of alkanes in emulsions was recently review by Herhold et al.[16]

2. Crystallization Kinetics in Droplets. Turnbull and coworkers have provided comprehensive details on the crystallization kinetics of liquid metals and alkane liquids.[6,7,17,18] In general, nucleation rates in emulsified samples can be determined by measuring the volume fraction of the solid (ϕ) as a function of time (t). The crystallization rate will be proportional to the volume fraction of droplets that contain no crystals ($1 - \varphi$) and, therefore, decreases with time:

$$\frac{\partial \phi}{\partial t} = k(1 - \varphi) \qquad (2)$$

For homogeneous volume nucleation, the rate constant k is proportional to the droplet volume. If nucleation proceeds at the droplet surface, k is proportional to the droplet surface. Solving eq 2 leads to the following expression that gives the volume fraction of solidified droplets as a function of time:

$$\phi = 1 - \exp(-kt), \qquad \text{or } \ln(1 - \varphi) = -kt \qquad (3)$$

That way, the values of k can be calculated.

In this contribution, we want to employ a new model system for the examination of the crystallization behavior in nanodroplets, namely, the so-called "miniemulsions".[19,20] Miniemulsions provide small, stable, and narrowly distributed nanodroplets with a controllable size (in the range of 50−500 nm) with partly adjustable surface tension and chemical surface structure. Mniemulsions are not defined by a size range, but more by a mode of operation and type of stabilization. Their highly reproducible generation by high-shear devices and the high stabilization by a combination of surfactants and osmotic-pressure-controlling agents (the growth of the nanodroplets can effectively be suppressed using an effective surfactant and a strong hydrophobe, which acts as an osmotic agent and stabilizes the system against Ostwald ripening), as well as some of their properties, were recently reviewed and are not discussed here in detail.[21]

The aim of this paper is to investigate the differences between the crystallization process in small miniemulsion droplets of defined, but variable, sizes, in comparison to the bulk material. As model systems, the crystallization of the hydrophobic hexadecane in direct miniemulsions and NaCl solution in inverse miniemulsions is studied as a function of several parameters, such as the droplet size and the interface tension.

Experimental Section

1. Materials. *n*-Hexadecane and sodium dodecyl sulfate (SDS), from Aldrich, and perfluorohexane, from Fluka, were used as received. The block copolymer emulsifier poly(butylene-*co*-ethylene)-*b*-poly(ethylene oxide) P(B-E)/PEO, consisting of a hydrophobic block (M_w = 3700 g·mol^{-1}) and a hydrophilic block (M_w = 3600 g·mol^{-1}), was synthesized starting from Kraton L (Shell) dissolved in toluene by adding ethylene oxide under the typical conditions of anionic polymerization. Isopar M (an isoparaffinic hydrocarbon) was supplied as a gift from Exxon Chemical.

2. Miniemulsion Preparation. 2.1. Preparation of the Direct Miniemulsions. A 6 g sample of *n*-hexadecane and 250 mg of perfluorohexane were mixed and added to a solution of 100 mg of SDS in 24 g of water. After stirring for 1 h, the miniemulsion was prepared by ultrasonicating the emulsion with a Branson model W450 sonifier ($^1/_2$-in. tip) at an amplitude of 90%. To prevent a temperature rise in the sample, the emulsion was ice-cooled.

2.2. Preparation of the Inverse Miniemulsions. A 1 g NaCl solution (0.1 M) was added to a solution of 100 mg of P(B-E)/PEO and 10 g of Isopar M. After the mixture was stirred for 1 h, the miniemulsion was prepared by ultrasonicating the emulsion with a Branson model W450 sonifier at 90% intensity under ice cooling.

3. Analytical Methods. The particle sizes were measured using a Nicomp particle sizer (Model 370, PSS Santa Barbara, USA) at a fixed scattering angle of 90°. For the measurements, the miniemulsions were highly diluted with the continuous phase (water or Isopar M, respectively).

The DSC measurements were conducted using a Netzsch model DSC 200 thermal analyzer. The measurements were conducted in two different modes: the scanning mode and the isothermal mode. In the first type of measurement, the heat evolved by a sample as it was cooled or heated at a constant rate was measured. In the second measurement, the heat evolved was recorded as a function of time when a sample was held at a fixed temperature. For both types, sample masses of 10−20 mg were used. For the scanning method, which was used in case of the direct miniemulsion system, the sample was cooled by liquid nitrogen from 30 °C to −10 °C, held for 2 min, and then heated to 30 °C. In case of the inverse miniemulsion system, the sample was cooled from room temperature to −60 °C, held at that temperature for 2 min, and then heated to room temperature. Cooling and heating rates of 5 K·min^{-1} were used for all measurements.

For the isothermal method, the sample was cooled to −2 °C, held for 1 min, and then cooled quickly (30 K·min^{-1}) to −5 °C and held at that point for 5 min to enable full droplet crystallization.

For comparison reasons, the bulk measurements were conducted on a hexadecane/perfluorohexane mixture (2.7 mol % perfluorohexane) and an aqueous NaCl solution (0.1 M), which, in both cases, is identical to the droplet composition.

The surface and interfacial tension measurements were performed with the Krüss model K12 processor tensiometer, using the DuNöuy-Ring method. The radius of the Pt−Ir ring RI12 was 9.545 mm, and the wire had a radius of 0.185 mm.

The wide-angle X-ray (WAXS) diffraction of the direct miniemulsion samples was measured at −5 °C (e.g., below the crystallization temperature of the hexadecane droplets), as well

TABLE 1: Characteristics of the Direct Miniemulsion Systems

sample	diameter (nm)	crystallization point (°C)	melting point (°C)	number of droplets per liter[a]
direct-1	410	−3.2	19.1	0.68×10^{16}
direct-2	326	−3.6	19.1	1.4×10^{16}
direct-3	308	−3.9	18.9	1.6×10^{16}
direct-4	276	−4.0	18.7	2.2×10^{16}
direct-5	241	−4.5	18.5	3.3×10^{16}
direct-6	218	−4.7	18.4	4.5×10^{16}
direct-7	183	−4.8	18.3	7.6×10^{16}
direct-8	167	−4.9	18.3	10.0×10^{16}
direct-9	136	−5.0	18.2	18.5×10^{16}

[a] For 20 wt % hexadecane in water.

as the bulk hexadecane for the direct system. For the inverse system, the WAXS measurements were performed below the crystallization temperature of the droplets (as verified by DSC), as well as for the bulk water (NaCl solution). As in the case of the DSC measurements, the bulk measurements were conducted on hexadecane/perfluorohexane mixtures and aqueous NaCl solutions.

Results and Discussion

1. Direct Miniemulsion Systems. In a first set of experiments, direct miniemulsions were prepared; these miniemulsions consisted of hexadecane as a dispersed phase, perfluorohexane as an ultrahydrophobe, SDS as a surfactant, and water as the continuous phase. The droplet size was varied, using different ultrasonication times. Measurement of the droplet size is a very difficult task; therefore, the droplet sizes in miniemulsions were characterized by cooling the miniemulsions, to solidify the droplets, resulting in the particle diameters shown in Table 1. In all cases, only one particle size with a Gaussian distribution and a standard deviation of <10% was achieved. Although hexadecane is added as an ultrahydrophobe in many literature known recipes, pure hexadecane miniemulsions still show Ostwald ripening, which is due to the absence of a counteracting osmotic force. Therefore, a third component, with a lower water solubility than hexadecane, is needed to stabilize the hexadecane miniemulsion osmotically. We have chosen perfluorohexane as an effective ultrahydrophobe for hexadecane, because perfluorohexane only weakly perturbs the crystallization process. The surface tensions of the miniemulsions are, in all cases, well above the value that is obtained after reaching the critical micelle concentration (cmc) of SDS (35 $mN \cdot m^{-1}$), indicating that, indeed, no free micelles are present in the system.

DSC measurements were used to investigate the dynamical crystallization temperature of the hexadecane. It is important to note that the continuous phase, the water, is not frozen under the measurement conditions (cooling to −10 °C). Figure 1 shows the DSC curves for hexadecane in bulk and for the miniemulsion with hexadecane in droplets (sample direct-6, particle size of 218 nm). To be able to compare the systems, the bulk hexadecane also contained the same amount of perfluorohexane as the hexadecane in the miniemulsion droplets (2.7 mol %). The addition of perfluorohexane is expected to depress the (static) melting point only by 0.362 K (calculated with $\Delta H_m = 53.8$ $kJ \cdot mol^{-1}$, $T_m = 18.4$ °C). Heating up the samples with crystallized droplets results in a slight decrease of the (dynamic) melting point in the droplets of 0.7 °C, from 19.1 °C to 18.4 °C. The temperature at which (dynamic) crystallization of hexadecane in the miniemulsion occurs is much lower than that in bulk hexadecane; it was strongly shifted from 12 °C in bulk to approximately −4 °C in the miniemulsion. This observation

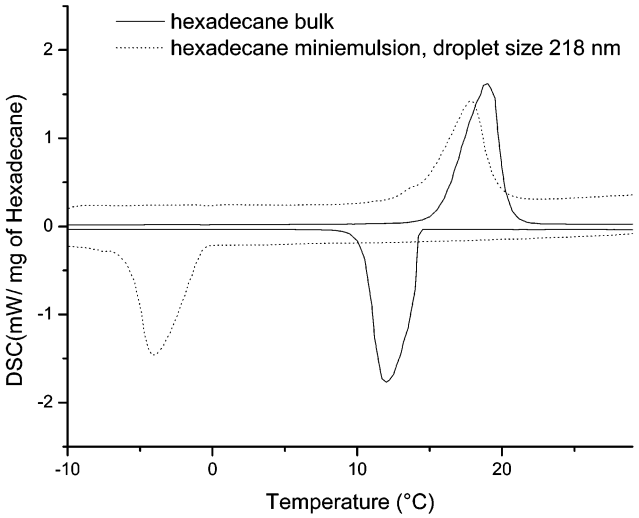

Figure 1. Comparison of the crystallization and melting behaviors of bulk hexadecane and hexadecane miniemulsion droplets in water (sample, direct-6; droplet size, 218 nm), as determined by DSC. Cooling and heating rates were 5 $K \cdot min^{-1}$.

means that the dynamic crystallization is influenced much more than the melting process. Kinetic retardation of crystallization in the droplets as a source of this effect can be excluded by a simple variation of the undercooling protocol. When the miniemulsion was cooled to 5 or 0 °C and held at the chosen temperature for 24 h, no crystallization in the droplets was observed. Please also note that that integrated value of the crystallization enthalpy corresponds well to the amount of hexadecane in the sample and, therefore, indicates full crystallization.

In the bulk system, a few nuclei are sufficient to induce (heterogeneous) nucleation, followed by crystal growth. In miniemulsion, $10^{16}-10^{17}$ sites per liter must nucleate separately, and crystal growth is limited to the dimension of the droplet. As already stated, the probability of nanodroplets to contain a "foreign" element (not hexadecane) acting as a substrate for heterogeneous nucleation is practically zero. This shifts the mechanism from heterogeneous nucleation to homogeneous nucleation.

The DSC scans of miniemulsions with different droplets sizes are shown in Figure 2a. In general, the crystallization temperature decreases with miniemulsion droplet size (also see Table 1); for instance, the maximum crystallization temperature for a miniemulsion with an average droplet size of ca. 400 nm is −3.2 °C, whereas at smaller droplets sizes of ca. 200 nm, the crystallization temperature is ca. −4.7 °C. It should be noted that all DSC scans were performed at the same cooling rate (5 $°C \cdot min^{-1}$) and, therefore, the effect of cooling rate on crystallization temperatures, which is very strong, can be disregarded. The high stability of the measurements is also indicated by the small fluctuations seen in the plot of the maximum of crystallization temperature versus the droplet sizes, which shows linear behavior (Figure 2b). The fact that the extrapolation for $1/d$ to a value of 0 (which represents the bulk material) leads to a crystallization temperature of −1 °C, far away from the measured 12 °C, again clearly indicates a change of nucleation mechanism from heterogeneous nucleation in the bulk to homogeneous nucleation in the droplets. The fact that smaller droplets rely on higher undercooling is also a direct consequence of homogeneous nucleation and the underlying Cahn-Hilliard mechanism:[22,23] smaller droplets rely on smaller wavelengths

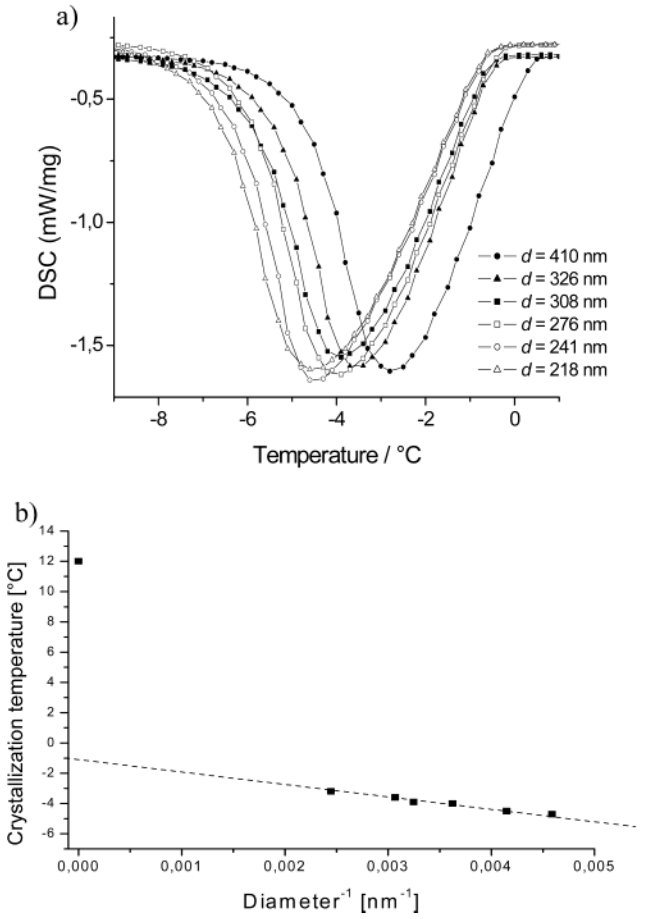

Figure 2. (a) Plot of the crystallization temperature against the particle size for the direct system. (b) Plot of the maximum crystallization temperature versus the droplet size.

of the chemical potential, which are stabilized only by a deeper temperature quench.

To be sure that the crystallization behavior in the droplets is not influenced by interactions between the droplets, and that, indeed, each droplet nucleates separately, samples with the same droplet sizes, but different droplet concentrations, were prepared. Indeed, the DSC curves of these samples did not show any dependency of the number of droplets on the crystallization temperature, which indicates the independence of each droplet and no influence by other droplets.

Another potential reason for a change in the crystallization temperature is the thermodynamic influence of the interfacial tension between the droplets and the continuous phase. This can be analyzed in excellent fashion, because miniemulsions allow one to easily change the interfacial tension without changing the droplet size by post-titrating with surfactant.[24] After the miniemulsion had been prepared, SDS was added stepwise, to decrease the surface tension and the connected droplet interfacial tension while keeping the droplet size constant. Figure 3 shows a plot of the *surface* tension of the miniemulsion (γ, in units of mN·m^{-1}) against the SDS concentration. A *surface* tension of 70 mN·m^{-1} is connected to droplets with a very low surfactant coverage and an *interfacial* tension of 38 mN·m^{-1} (this value has been independently measured by a interfacial tension measurement on a plane interface of hexadecane and water); a *surface* tension of 35 mN·m^{-1} represents droplets that are fully covered by surfactant and corresponds to a *interfacial* tension of 8.7 mN·m^{-1} (also independently determined between hexadecane and aqueous SDS solution at the cmc concentration). The DSC curves for the samples with different surface tensions

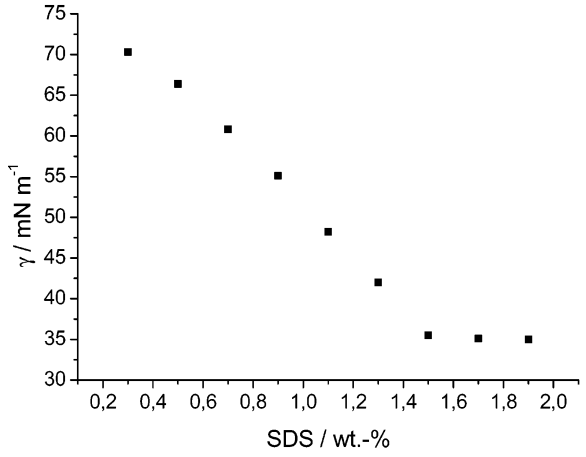

Figure 3. Surface tension of the miniemulsion versus the SDS concentration (wt. %). Sample conditions were as follows: sample, direct-6; droplet size, 218 nm; solids content of hexadecane in water, 20%.

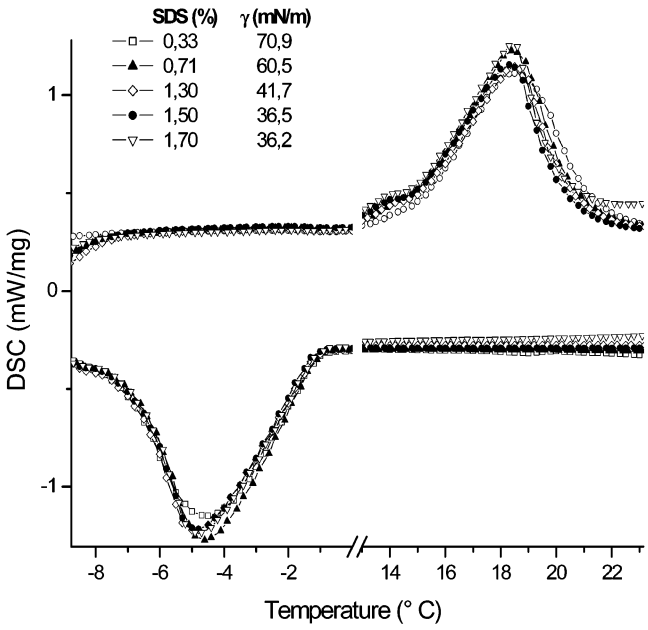

Figure 4. DSC curves for miniemulsions with the same droplet size but different interfacial tensions between the hexadecane droplets and the continuous phase.

are shown in the Figure 4. As can be seen, after a miniemulsion with droplets of a defined size has been created, the interfacial tension between the continuous and the dispersed phase does not play any role in the changing the crystallization or melting temperature of the droplets, even for the maximal changes as demonstrated in this set of experiments. This result has several important implications for the physical chemistry of such nanodroplets:

(1) The Gibbs−Thomson reaction has (still) no importance in this range of droplet sizes. This is not trivial because a surface might influence the crystallization thermodynamically, to a certain depth.

(2) There is also no influence of a droplet or Kelvin pressure on the crystallization behavior, at least in this range of droplet sizes or surface sites.

(3) Nucleation from the surfactant layer can again be excluded.

To analyze the crystallization behavior in detail, closer examination of the DSC exotherm is necessary. Typical DSC

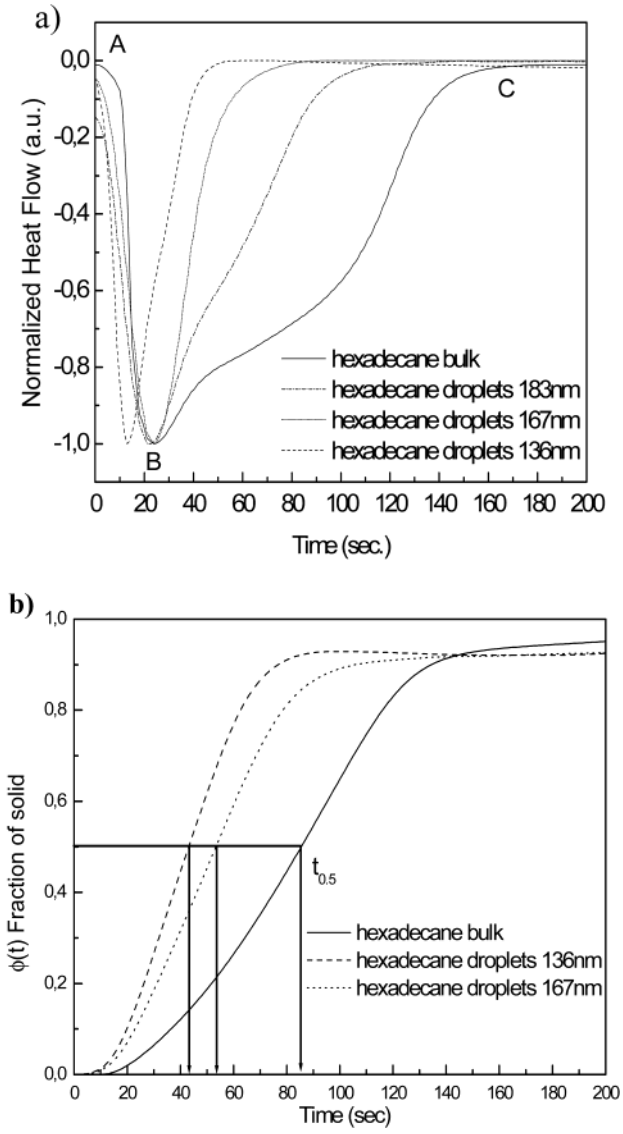

Figure 5. (a) Crystallization exotherms for isothermal crystallization of hexadecane in miniemulsions of different droplets size and of bulk hexadecane. (b) Half-time of crystallization, $t_{0.5}$, for bulk hexadecane and hexadecane droplets 136 and 167 nm in size.

crystallization exotherms for isothermal crystallization of hexadecane in miniemulsions of different droplets sizes (183, 176, and 136 nm) and of bulk hexadecane are compared in Figure 5a. (All DSC spectra are normalized to bulk hexadecane crystallization.) Crystallization is assumed to begin at point A, which is preceded by a short period, presumably because of the required thermal equilibration. An increasing heat flow due to evolution of the enthalpy of crystallization is evident until a maximum is observed at point B. The rate of evolution of the enthalpy of crystallization depends strongly on the kinetics of the crystallization process, which is very sensitive to changes in the crystallization temperature. After point B, crystallization slows significantly, and the measurement is terminated (i.e., at point C) when no noticeable change in the heat flow is detected any further.

An important parameter that can be measured from Figure 5a is the half time of crystallization, $t_{0.5}$, which is defined as the time from the onset of the crystallization to the point where the crystallization is 50% complete (see Figure 5b). As can be seen from Figure 5, the crystallization rate in the droplets of the miniemulsion (as reflected in the $t_{0.5}$ values) is higher than

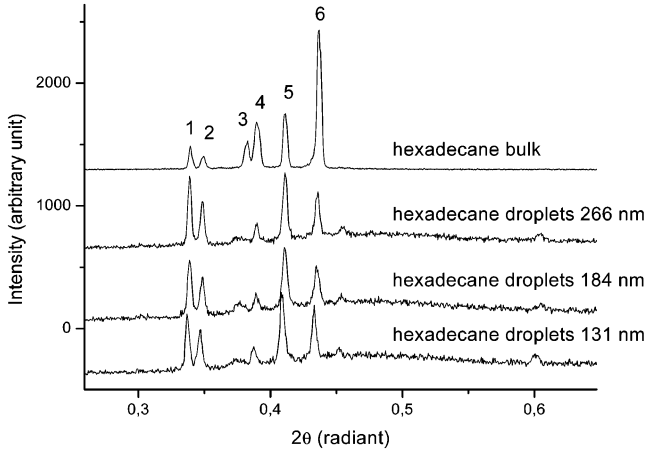

Figure 6. X-ray diffraction patterns of bulk hexadecane and miniemulsions with different particle sizes; (*hkl*) interference peaks are noted (1, (010); 2, (011); 3, (101); 4, (013); 5, (111); 6, (110)).

that for the bulk. The value of $t_{0.5}$ for miniemulsion droplets with a size of ca. 140 nm is as short as 42 s, whereas, for the bulk case, $t_{0.5} \approx 85$ s. One possible explanation for this effect is an increase of the rate constant with decreasing droplet size. Another explanation for this behavior, however, is that the heat which is evolved during crystallization can be transported much better from smaller droplets with a large surface to the water medium, which is acting as a heat bath. Attempts to fit the crystallization rate to homogeneous or heterogeneous nucleation (by plotting the rate constant k versus the droplet surface or droplet volume) did not result in a simple relationship, illustrating the importance of heat-flow effects.

WAXS measurements have been used to analyze the crystals formed in bulk hexadecane and in hexadecane nanodroplets (under confined conditions). Figure 6 shows the X-ray diffraction patterns for the bulk hexadecane and the miniemulsions with different particle sizes. The bump in the case of the miniemulsions can be attributed to the fact that the dispersion containing water is measured. The positions of the peaks are slightly shifted to smaller values, indicating an expansion of the crystals in the droplets, compared to the crystals obtained in bulk. The relative peak intensity ratios show major changes, and additional weak peaks are appearing, which is indicative of a change of the crystal shape and a slight distortion of crystal symmetry within the nanodroplets. Therefore, the crystal morphology does,indeed, react sensitively to the droplet confinement. The changes in melting behavior are only practically nonexistent; therefore, these changes mainly concern the crystal superstructure.

2. Inverse System. For the preparation of aqueous nanodroplets in a continuous oily environment (inverse miniemulsions), 0.1 M NaCl aqueous solution was miniemulsified in Isopar M. By increasing the time of sonication, different droplet sizes were created. The hydrophilic salt NaCl, which is completely insoluble in the continuous phase, is used as the osmotic control agent. The characteristics of the examined inverse miniemulsions are summarized in Table 2.

The melting points must be visible, in view of the fact that the water crystallizing from salt solutions is practically free of salt (as icebergs); i.e., the melting is the melting of bare ice in the presence of a high-salt-containing droplet, which is a complicated redissolution phenomenon. In the smallest droplets, ~33 000 NaCl molecules are pressed out of the water crystals, presumably forming a separate nanophase. This is why, for the

TABLE 2: Characteristics of the Inverse Miniemulsions

	droplet size (nm)	crystallization point (°C)	melting point (°C)	number of droplets per liter[a]
inverse-1	330	−44.6	−0.8	0.13×10^{17}
inverse-2	257	−45.0	−0.7	0.27×10^{17}
inverse-3	191	−45.8	−0.5	0.67×10^{17}
inverse-4	133	−46.3	−1.0	1.98×10^{17}
inverse-5	109	−46.6	−1.1	3.65×10^{17}

[a] For a 20 wt % dispersion of 0.1 M NaCl solution in Isopar M.

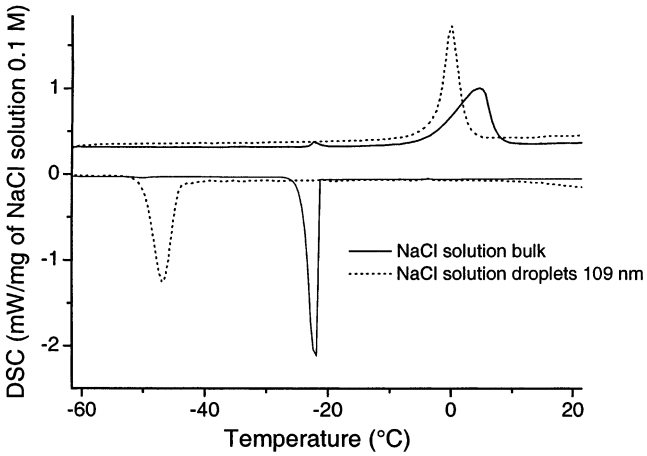

Figure 7. Comparison between bulk water (NaCl solution 0.1 M) and the inverse miniemulsion. Cooling and heating rates were 5 K·min^{-1}.

water nanodroplets, we focus only on the undercooling and freezing behavior.

DSC indicates a strong shifting of the dynamic crystallization temperature from the bulk NaCl solution (251 K) to the droplets (227−229 K), as shown in Figure 7 for the 109-nm droplets. This is again related to the change of the nucleation mechanism, from heterogeneous to homogeneous nucleation, in each individual droplet. For the inverse miniemulsion, the dynamic crystallization temperature again is shifting with the droplet size (Figure 8). This means that the effects previously described do not depend on the chemical nature of the material in the droplet: The wavelength of chemical potential required for homogeneous nucleation is simply smaller for smaller droplets.

However, the structure of the water crystals sensitively reacts toward the liquid confinement and shows some interesting peculiarities. Figure 9a compares the WAXS spectra of ice crystals grown from bulk NaCl solution and from the corresponding nanodroplets. In any case, a hexagonal ice structure is detected, making crystallization in liquid nanodroplets different from corresponding experiments in mesoporous solids.[4] Interestingly, although taken clearly from an isotropic dispersion state, the ratios of peak-intensity ratios differ between the bulk and the droplet experiments. It is obvious that all the peaks with a *z*-component are significantly decreased or even eliminated for the droplets, indicating that the ice nanocrystals do grow just weakly in the *z*-direction.

The question of whether this restriction to an almost-two-dimensional shape is typical for the primary nuclei of homogeneously nucleated ice from saltwater or just induced by the nanodroplet starting situation can be speculated; however, we strongly favor the first explanation.

From the WAXS data, the average size (L) of the crystallites was estimated from the integral widths B_{hkl} of the (hkl) reflections, using the Scherrer equation in the form $L_{hkl} = \lambda/(B_{hkl} \cos \theta_{hkl})$, where the integral width is used (in units of radians). The integral widths of the single reflections were obtained from the WAXS data after subtraction of the scattering from the dispersion agent, Isopar M. Taking into account the instrumental resolution, our WAXS setup allows us to determine crystallite sizes up to 80 nm.[25]

The evaluation of (hkl) peaks (110) and (102) are exemplarily shown in Figure 9b. Expectedly, the (110) peak gives a larger L value than does the (102) peak, which contains a weak *z*-component, again suggesting a rather flat crystal shape. For all peaks, it is found that the crystallite size decreases as the droplet size increases. In the 90-nm droplets, crystallites with an in-plane L_{100} value of ∼50 nm were found, whereas for 490-nm droplets, the crystallites show a size of only ∼25 nm. The crystal size of the heterogeneously nucleated water is expectedly very large, i.e., beyond instrumental resolution.

The ice nanocrystals are, in all cases, smaller than the droplets, which provides nonrupture and droplet stability also in the frozen case. This is not true for all materials showing a pronounced tendency toward one- or two-dimensional crystallization, e.g., naphthalene. This also means that, in all cases, more than one nucleation site is present in every droplet, presumably a consequence of the spinodal crystallization mechanism that generates wavelike patterns of nuclei simultaneously.

The number of crystals per unit volume depends on the ratio v_{nucl}/v_{growth} (velocity of nucleation/velocity of growth); therefore, smaller droplets show either a decreased v_{nucl} value and/or an increased v_{growth} value. Assisted by the kinetic data, it is nearby

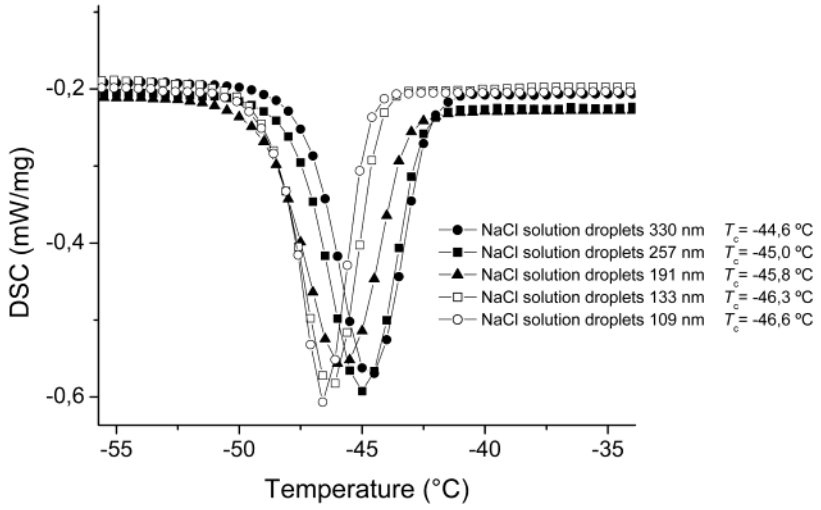

Figure 8. Dependence of the crystallization temperature on the droplet size in the inverse system.

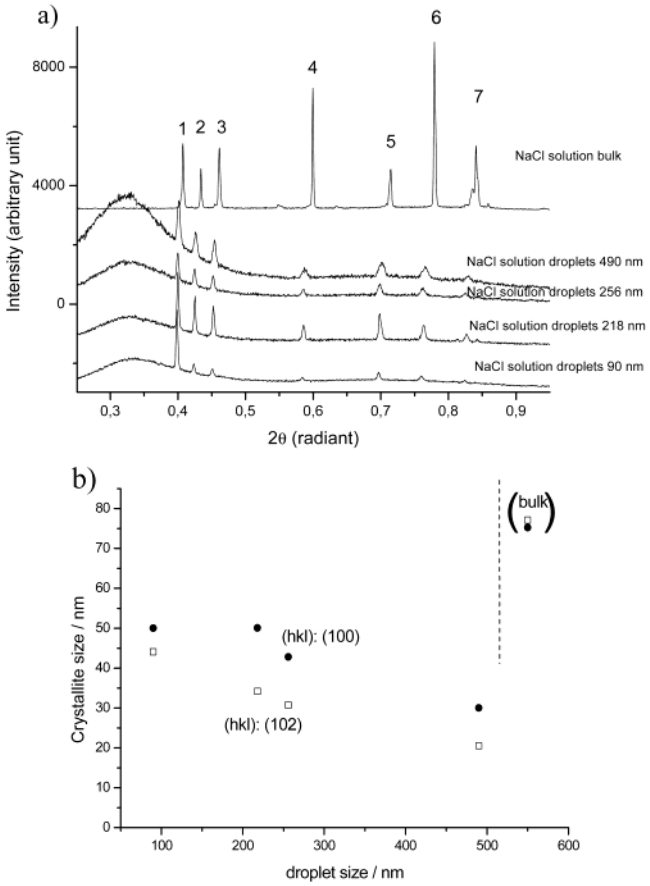

Figure 9. (a) Wide-angle X-ray spectra for bulk water and water droplets of different sizes; (*hkl*) interference peaks are noted (1, (100); 2, (002); 3, (101); 4, (102); 5, (110); 6, (103); 7, (200); 8, (112)). (b) Evaluation of the (*hkl*) peaks (110) and (102).

to assume that, indeed, it is the rate of homogeneous nucleation that is smaller for the smaller droplets, although heat-flow effects also cannot be excluded.

Conclusion

Dynamic crystallization and melting experiments were performed in small, stable, and narrowly distributed nanodroplets of miniemulsions. Both regular and inverse systems were examined, characterizing, first, the crystallization of hexadecane and second, the crystallization of ice. It was shown for both cases that the temperature of crystallization in such droplets is significantly decreased (or the required undercooling is increased), as compared to the bulk material. This was attributed to a very effective suppression of heterogeneous nucleation. This means that crystallization does not occur in the bimodal region of the phase diagram, but much deeper below the spinodal line, which increases the region of metastability by another 25 K. This is important for an entire variety of technical applications.

Interestingly, it was also found that the required undercooling also depends on the nanodroplet size: The undercooling increases as the droplet size decreases. This can be understood by the approach that smaller droplets rely on smaller spinodal fluctuation of the chemical potential, which, again, are generated by deeper temperature quenches.

Interestingly, the confinement in droplets also influences the crystal morphology and crystal structure, as detected by X-ray analysis. The more-plastic hexadecane crystals show a slight shift of the peaks and the occurrence of extra, symmetry-forbidden peaks, suggesting a distortion of the crystal structure by the adaptation to the almost-spherical shape. Water, on the other hand, shows the same hexagonal structure, but the relative peak intensities change greatly, suggesting a very flat shape of ice nanocrystals. At the same time, more than one ice crystal nucleates in each nanodroplet, making the crystalline nanodroplet superstructure potentially resemble a stack of pancakes. The nanocrystal size in the case of ice increases as the droplet size decreases, which can be due to heat-flow effects, a decreased nucleation rate, or even a better packing of the nanocrystals in smaller droplets.

Future work will be focused on a structural analysis of the resulting crystal structures by microscopic techniques, as well as an expansion of the nanodroplet experiments to molecules with functionality, e.g., dye molecules or liquid crystals.

Acknowledgment. We thank Dr. Bernd Smarsly and Ingrid Zenke for the X-ray measurements.

References and Notes

(1) Vanfleet, R. R.; Mochel, J. M. *Surf. Sci.* **1995**, *341*, 40.
(2) Kaneko, N.; Horie, T.; Ueno, S.; Yano, J.; Katsuragi, T.; Sato, K. *J. Cryst. Growth* **1999**, *197*, 263.
(3) McClements, D. J.; Dickinson, E.; Dungan, S. R.; Kinsella, J. E.; Ma, J. G.; Povey, M. J. W. *J. Colloid Interface Sci.* **1993**, *160*, 293.
(4) Schreiber, A.; Ketelsen, I.; Findenegg, G. H. *Phys. Chem. Chem. Phys.* **2001**, *3*, 1185.
(5) Vonnegut, B. *J. Colloid Sci.* **1948**, *3*, 563.
(6) Turnbull, D. *J. Chem. Phys.* **1952**, *20*, 411.
(7) Turnbull, D.; Cormia, R. L. *J. Chem. Phys.* **1961**, *34*, 820.
(8) Kelton, K. F. In *Solid State Physics: Advances in Research and Applications*; Ehrenreich, H., Turnbull, D. Eds.; Academic: New York, 1991.
(9) Milhofer, H. F.; Garti, N.; Kamyshny, A. *J. Cryst. Growth* **1999**, *199*, 1365.
(10) Yano, J. F.; Milhofer, H.; Wachtel, E.; Garti, N. *Langmuir* **2000**, *16*, 10005.
(11) Charoenrein, S.; Reid, D. S. *Thermochim. Acta* **1989**, *156*, 373.
(12) McClements, D. J.; Dungan, S. R.; German, J. B.; Simoneau, C.; Kinsella, J. E. *J. Food Sci.* **1993**, *58*, 1148.
(13) Walstra, P.; Berensteyn, E. C. H. *Neth. Milk Dairy J.* **1975**, *29*, 35.
(14) McClements, D. J.; Dickinson, E.; Povey, M. J. W. *Chem. Phys. Lett.* **1990**, *172*, 449.
(15) Dickinson, E.; Kruizenga, F. J.; Povey, M. J. W.; Molen, M. V. D. *Colloids Surf. A* **1993**, *81*, 273.
(16) Herhold, A. B.; Ertas, D.; Levine, A. J.; King, H. E. *Phys. Rev. E* **1999**, *59*, 6946.
(17) Turnbull, D. *J. Appl. Phys.* **1950**, *21*, 1022.
(18) Turnbull, D. *J. Chem. Phys.* **1952**, *20*, 411.
(19) Landfester, K.; Bechthold, N.; Tiarks, F.; Antonietti, M. *Macromolecules* **1999**, *32*, 5222.
(20) Landfester, K. *Macromol. Symp.* **2000**, *150*, 171.
(21) Landfester, K. *Macromol. Rapid Commun.* **2001**, *22*, 896.
(22) Cahn, J. W.; Hilliard, J. E. *J. Chem. Phys.* **1958**, *28*, 258.
(23) Cahn, J. W.; Hilliard, J. E. *J. Chem. Phys.* **1959**, *31*, 688.
(24) Landfester, K.; Bechthold, N.; Tiarks, F.; Antonietti, M. *Macromolecules* **1999**, *32*, 2679.
(25) Cullity, D. *Elements of X-ray Diffraction*; Addison-Wesley: Reading, MA, 1978.